Evidence from South Africa for a protracted end-Permian extinction on land

Pia A. Viglietti[a,b,1], Roger B. J. Benson[b,c], Roger M. H. Smith[b,d], Jennifer Botha[e,f], Christian F. Kammerer[g], Zaituna Skosan[d], Elize Butler[e], Annelise Crean[d], Bobby Eloff[e], Sheena Kaal[d], Joël Mohoi[e], William Molehe[e], Nolusindiso Mtalana[d], Sibusiso Mtungata[d], Nthaopa Ntheri[e], Thabang Ntsala[e], John Nyaphuli[e], Paul October[d], Georgina Skinner[d], Mike Strong[d], Hedi Stummer[d], Frederik P. Wolvaardt[b], and Kenneth D. Angielczyk[a,b]

[a]Negaunee Integrative Research Center, Field Museum of Natural History, Chicago, IL 60605; [b]Evolutionary Studies Institute, University of the Witwatersrand, Johannesburg, 2050, South Africa; [c]Department of Earth Sciences, University of Oxford, Oxford OX1 3AN, United Kingdom; [d]Karoo Palaeontology, Iziko South African Museum, Cape Town, 8001, South Africa; [e]Department of Zoology and Entomology, University of the Free State, Bloemfontein, 9300, South Africa; [f]Karoo Palaeontology, National Museum, Bloemfontein, 9300, South Africa; and [g]Paleontology, North Carolina Museum of Natural Sciences, Raleigh, NC 27601

Edited by Anna K. Behrensmeyer, Smithsonian National Museum of Natural History, Washington, DC, and approved March 2, 2021 (received for review August 12, 2020)

Earth's largest biotic crisis occurred during the Permo–Triassic Transition (PTT). On land, this event witnessed a turnover from synapsid- to archosauromorph-dominated assemblages and a restructuring of terrestrial ecosystems. However, understanding extinction patterns has been limited by a lack of high-precision fossil occurrence data to resolve events on submillion-year timescales. We analyzed a unique database of 588 fossil tetrapod specimens from South Africa's Karoo Basin, spanning ∼4 My, and 13 stratigraphic bin intervals averaging 300,000 y each. Using sample-standardized methods, we characterized faunal assemblage dynamics during the PTT. High regional extinction rates occurred through a protracted interval of ∼1 Ma, initially co-occurring with low origination rates. This resulted in declining diversity up to the acme of extinction near the *Daptocephalus–Lystrosaurus declivis* Assemblage Zone boundary. Regional origination rates increased abruptly above this boundary, co-occurring with high extinction rates to drive rapid turnover and an assemblage of short-lived species symptomatic of ecosystem instability. The "disaster taxon" *Lystrosaurus* shows a long-term trend of increasing abundance initiated in the latest Permian. *Lystrosaurus* comprised 54% of all specimens by the onset of mass extinction and 70% in the extinction aftermath. This early *Lystrosaurus* abundance suggests its expansion was facilitated by environmental changes rather than by ecological opportunity following the extinctions of other species as commonly assumed for disaster taxa. Our findings conservatively place the Karoo extinction interval closer in time, but not coeval with, the more rapid marine event and reveal key differences between the PTT extinctions on land and in the oceans.

Mass extinction | Permo-Triassic | Diversity dynamics | *Lystrosaurus* | Karoo Basin

Mass extinctions are major perturbations of the biosphere resulting from a wide range of different causes including glaciations and sea level fall (1), large igneous provinces (2), and bolide impacts (3, 4). These events caused permanent changes to Earth's ecosystems, altering the evolutionary trajectory of life (5). However, links between the broad causal factors of mass extinctions and the biological and ecological disturbances that lead to species extinctions have been difficult to characterize. This is because ecological disturbances unfold on timescales much shorter than the typical resolution of paleontological studies (6), particularly in the terrestrial record (6–8). Coarse-resolution studies have demonstrated key mass extinction phenomena including high extinction rates and lineage turnover (7, 9), changes in species richness (10), ecosystem instability (11), and the occurrence of disaster taxa (12). However, finer time resolutions are central to determining the association and relative timings of these effects, their potential causal factors, and their interrelationships. Achieving these goals represents a key advance in understanding the ecological mechanisms of mass extinctions.

The end-Permian mass extinction (ca. 251.9 Ma) was Earth's largest biotic crisis as measured by taxon last occurrences (13–15). Large outpourings from Siberian Trap volcanism (2) are the likely trigger of calamitous climatic changes, including a runaway greenhouse effect and ocean acidification, which had profound consequences for life on land and in the oceans (16–18). An estimated 81% of marine species (19) and 89% of tetrapod genera became extinct as established Permian ecosystems gave way to those of the Triassic. In the ocean, this included the complete extinction of reef-forming tabulate and rugose corals (20, 21) and significant losses in previously diverse ammonoid, brachiopod, and crinoid families (22). On land, many nonmammalian synapsids became extinct (16), and the glossopterid-dominated floras of Gondwana also disappeared (23). Stratigraphic sequences document a global "coral gap" and "coal gap" (24, 25), suggesting reef and forest ecosystems were rare or absent for up to 5 My after the event (26). Continuous fossil-bearing deposits documenting patterns of turnover across the Permian–Triassic transition (PTT) on land (27)

Significance

Mass extinctions permanently altered life's evolutionary trajectory five times in Earth's history, and the end-Permian extinction was the greatest of these biotic crises. South Africa's unparalleled fossil record provides a window into mass extinction dynamics on land. We analyze a unique dataset comprising hundreds of precisely positioned tetrapod fossils, identifying a protracted (∼1 Ma) extinction. This contrasts with the rapid marine extinction, demonstrating that the effects of biotic crises vary prominently among Earth's surface environments. We also identify the blooming of "disaster taxa" before the main extinction rather than in its aftermath as assumed previously. These changes contributed to breaking the incumbency of previously dominant mammal relatives (synapsids) after the extinction and to the Triassic rise of crocodile- and dinosaur-line archosaurs.

Author contributions: P.A.V., R.B.J.B., and K.D.A. designed research; P.A.V., R.B.J.B., and K.D.A. performed research; P.A.V., R.M.H.S., J.B., C.F.K., Z.S., E.B., A.C., B.E., S.K., J.M., W.M., N.M., S.M., N.N., T.N., J.N., P.O., G.S., M.S., H.S., and F.P.W. contributed raw data/analytic tools; R.B.J.B. analyzed data; and P.A.V., R.B.J.B., and K.D.A. wrote the paper.

The authors declare no competing interest.

This article is a PNAS Direct Submission.

[1]To whom correspondence may be addressed. Email: pviglietti@fieldmuseum.org.

This article contains supporting information online at https://www.pnas.org/lookup/suppl/doi:10.1073/pnas.2017045118/-/DCSupplemental.

Published April 19, 2021.

and in the oceans (28) are geographically widespread (29, 30), including marine and continental successions that are known from China (31, 32) and India (33). Continental successions are known from Russia (34), Australia (35), Antarctica (36), and South Africa's Karoo Basin (Fig. 1 and 37–40), the latter providing arguably the most densely sampled and taxonomically scrutinized (41–43) continental record of the PTT. The main extinction has been proposed to occur at the boundary between two biostratigraphic zones with distinctive faunal assemblages, the *Daptocephalus* and *Lystrosaurus declivis* assemblage zones (Fig. 1), which marks the traditional placement of the Permian–Triassic geologic boundary [(37) but see ref. 44]. Considerable research has attempted to understand the anatomy of the PTT in South Africa (38, 39, 45–52) and to place it in the context of biodiversity changes across southern Gondwana (53, 54) and globally (29, 31, 32, 44, 47, 55).

Decades of research have demonstrated the richness of South Africa's Karoo Basin fossil record, resulting in hundreds of stratigraphically well-documented tetrapod fossils across the PTT (37, 39, 56). This wealth of data has been used qualitatively to identify three extinction phases and an apparent early post-extinction recovery phase (39, 45, 51). Furthermore, studies of Karoo community structure and function have elucidated the potential role of the extinction and subsequent recovery in breaking the incumbency of previously dominant clades, including synapsids (11, 57). Nevertheless, understanding patterns of faunal turnover and recovery during the PTT has been limited by the scarcity of quantitative investigations. Previous quantitative studies used coarsely sampled data (i.e., assemblage zone scale, 2 to 3 Ma time intervals) to identify low species richness immediately after the main extinction, potentially associated with multiple "boom and bust" cycles of primary productivity based on $\delta^{13}C$ variation during the first 5 My of the Triassic (41, 58). However, many details of faunal dynamics in this interval remain unknown. Here, we investigate the dynamics of this major tetrapod extinction at an unprecedented time resolution (on the order of hundreds of thousands of years), using sample-standardized methods to quantify multiple aspects of regional change across the *Cistecephalus*, *Daptocephalus*, and *Lystrosaurus declivis* assemblage zones.

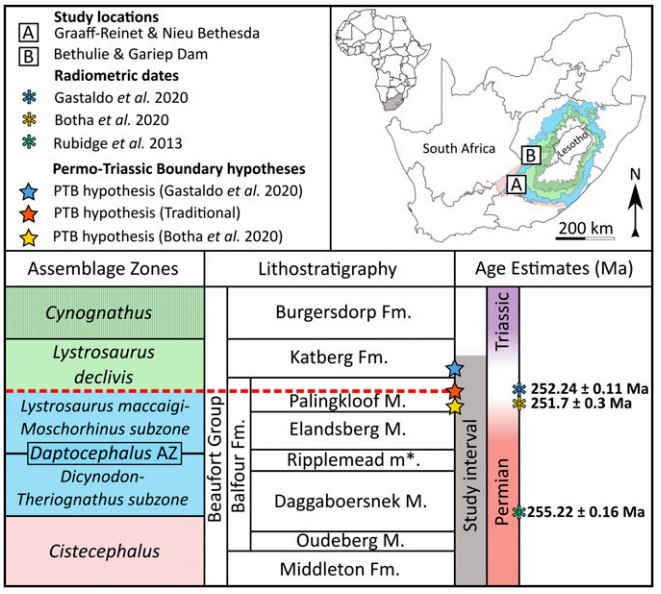

Fig. 1. Map of South Africa depicting the distribution of the four tetrapod fossil assemblage zones (*Cistecephalus*, *Daptocephalus*, *Lystrosaurus declivis*, *Cynognathus*) and our two study sites where fossils were collected in this study (sites A and B). Regional lithostratigraphy and biostratigraphy within the study interval are shown alongside isotope dilution–thermal ionization mass spectrometry dates retrieved by Rubidge et al., Botha et al., and Gastaldo et al. (37, 44, 80). The traditional (dashed red line) and associated PTB hypotheses for the Karoo Basin (37, 44) are also shown. Although traditionally associated with the PTB, the *Daptocephalus–Lystrosaurus declivis* Assemblage Zone boundary is defined by first appearances of co-occurring tetrapod assemblages, so its position relative to the three PTB hypotheses is unchanged. The Ripplemead member (*) has yet to be formalized by the South African Committee for Stratigraphy.

Results

We tracked multiple aspects of tetrapod extinction, origination, and regional diversity dynamics across the upper *Cistecephalus* (CAZ), *Daptocephalus* (DAZ), and *Lystrosaurus declivis* (LAZ) assemblage zones (Fig. 2 and Table 1) at high time resolution and alongside the relative abundances of the disaster taxon *Lystrosaurus*, comparing our results to the less complete data available from global terrestrial sections outside of South Africa (Fig. 3 *A*–*C*). We quantified extinction and origination rates, diversification, turnover, and evenness. Additionally, we present subsampled and other richness estimates for all bin intervals alongside face-value counts of species and diagnostic fossil occurrences (Fig. 4 *A*–*C*). Most of the important shifts in these variables occur between the *Lystrosaurus maccaigi-Moschorhinus* subzone (upper DAZ) and lower LAZ (upper Palingkloof Member and lower Katberg), spanning three stratigraphic bin intervals and suggesting an approximate extinction duration of ~1 Ma, with the main extinction acme occurring in an approximately <300,000 y time window above the DAZ–LAZ boundary.

Extinction, Origination, and Turnover. Regional extinction rates remain low in the earlier half of the study interval, with the exception of a slight increase at the boundary between the *Dicynodon-Theriognathus* (lower DAZ) and upper DAZ subzones of the DAZ. However, extinction becomes significantly elevated above background levels in the lower Palingkloof Member, before the main extinction acme. These elevated extinction rates co-occur with low origination rates, resulting in negative diversification for an interval of ~600,000 y (two bin intervals) before the DAZ–LAZ boundary. In total, extinction rate remains high over an interval estimated at ~900,000 y (three bin intervals). Most of the DAZ taxa go extinct in this interval, with extinction peaking in a single time bin just above the DAZ–LAZ boundary (<300,000 y, Fig. 3*A*). Extinction dynamics likely reflect the disappearance of theriodonts (*Aelurognathus*, *Cyonosaurus*, *Ictidosuchoides*), pareiasaurs (*Pareiasaurus*), cynodonts (*Cynosaurus*, *Vetusodon*), and dicynodont species (*Daptocephalus*, *Dicynodon*, *Dicynodontoides*, *Diictodon*, *Dinanomodon*, *Emydorhinus*, *Oudenodon*, *Pelanomodon*).

Regional origination is generally stable and low throughout the DAZ, with the exception of a minor uptick at the boundary between the lower and upper DAZ. We then observe a time-lagged pulse of high origination after the main extinction acme, occurring in the lower LAZ. Multiple new taxa appeared during this origination pulse, including archosauromorphs (*Prolacerta*, *Proterosuchus*) amphibians (*Lydekkerina*, *Micropholis*), cynodonts (*Galesaurus*, *Thrinaxodon*), dicynodonts (*Lystrosaurus declivis*, *Lystrosaurus murrayi*), parareptiles (*Saurodektes*), and therocephalians (*Ericiolacerta*, *Scaloposaurus*). High rates of both extinction and origination co-occur in the immediate extinction aftermath phase, resulting in positive diversification rates and high turnover. This had previously been referred to as a post extinction "recovery fauna" (37, 39) due to the appearance of several geologically short-lived taxa such as the archosauriform *Proterosuchus*, the cynodont *Progalesaurus*, and various therocephalians (*Ericiolacerta*, *Olivierosuchus*, *Regisaurus*) (Figs. 2 and 3*A*).

Richness and Evenness. Both subsampled richness estimates and counted richness values using several methods are greatest in the lowermost DAZ (Daggaboersnek Member, Fig. 4*C*). Data are insufficient for an accurate measurement of richness and

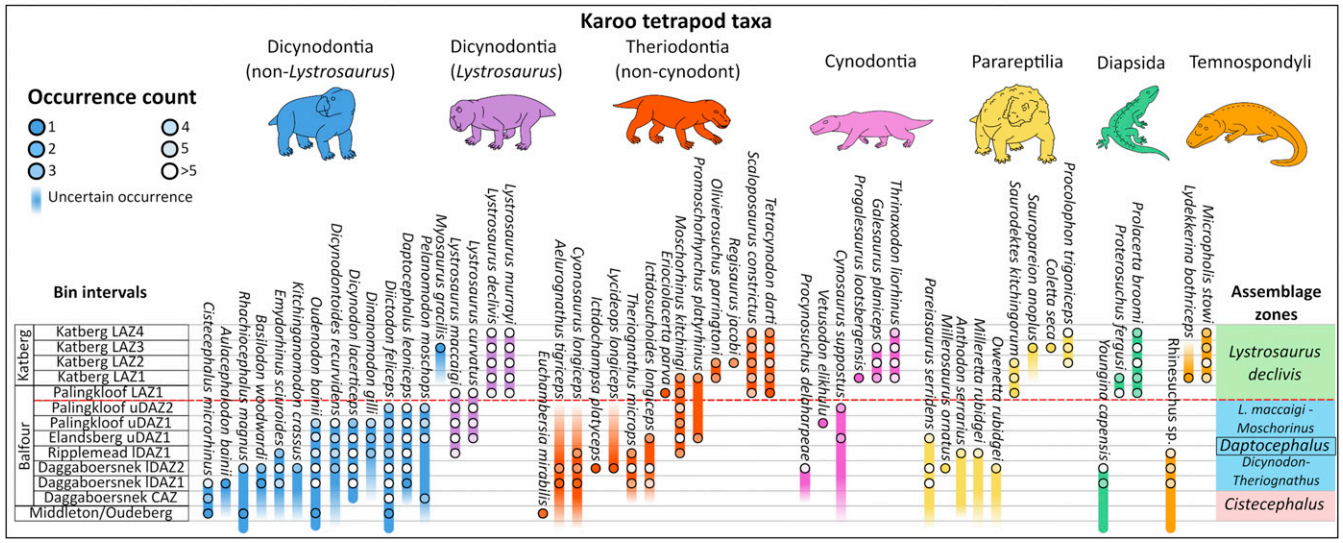

Fig. 2. Stratigraphic ranges of the 53 Karoo fossil tetrapod species included in this study with occurrence counts (infilled circles) in each bin interval. The dashed red line indicates the *Daptocephalus–Lystrosaurus declivis* Assemblage Zone boundary, the traditional PTB in the Karoo Basin. Some species have lower-resolution stratigraphic data, and these were included here (but not in the analyses) to show uncertain first or last occurrences for specific species in our study.

diversification for most strata of the underlying *Cistecephalus* Assemblage Zone, which requires in-depth stratigraphic and taxonomic study. However, if our finding of low species richness in the upper *Cistecephalus* Assemblage Zone is robust, it has intriguing implications for the overall species richness of the uppermost Karoo assemblage zones. The DAZ shows a pattern of declining richness that begins in the lowermost DAZ based on face-value species counts (Fig. 4*C*), or slightly later based on subsampled richness estimates and their estimated error terms, at the onset of increased extinction rates in the *Lystrosaurus maccaigi-Moschorhinus* subzone (Fig. 4*C*, uppermost Elandsberg Member). Richness remains low through the upper Palingkloof Member (lower LAZ). In the lower Katberg Formation, where we begin to see new species appear in the lower LAZ, high richness is obtained at our reported quorum level but not at lower quora (*SI Appendix*, Fig. S6) and is associated with relatively high estimation error, warranting further investigation. Our findings tentatively suggest fluctuations in richness during the earliest Triassic, which may be associated with primary productivity (41). We also demonstrate a preboundary interval of low richness, consistent with our findings of negative diversification rates preceding the DAZ–LAZ boundary (Fig. 3*A*) and with the hypothesized extinction phases of Smith and Botha-Brink (39).

Evenness is a measure of the distribution of relative abundances of the species in a stratigraphic interval. Our data show species-level evenness to be relatively stable throughout the *Cistecephalus* and *Daptocephalus* assemblage zones and across the main extinction acme close to the *Daptocephalus–Lystrosaurus declivis* Assemblage Zone boundary, likely because of the retention of some extinction acme-crossing species (*Lystrosaurus curvatus*, *Lystrosaurus maccaigi*, *Moschorhinus*, *Promoschorhynchus*) alongside the appearance of new species in the inferred recovery phase. Nevertheless, a clear decrease in species-level evenness is

Table 1. Upper stratigraphic bin interval boundaries (in meters) specimen counts and average specimens per meter for Site A (Graaff-Reinet, Nieu Bethesda) and Site B (Bethulie, Gariep Dam) study locations

Bin Interval	Site A upper boundary (m)	Site A specimen counts	Site A specimens per meter	Site B upper boundary (m)	Site B specimen counts	Site B specimens per meter	Total specimen counts
Katberg_*Lystrosaurus*-4	560	13	0.3	234	42	0.5	55
Katberg_*Lystrosaurus*-3	520	4	0.8	155	54	3.3	58
Katberg_*Lystrosaurus*-2	515	2	0.4	138.75	58	3.6	60
Katberg_*Lystrosaurus*-1	510	15	1.5	122.5	49	1.5	64
Palingkloof_*Lystrosaurus*-1	500	13	0.7	90	28	2.8	41
Palingkloof_u*Daptocephalus*-2	482	13	1.6	80	15	4.5	28
Palingkloof_u*Daptocephalus*-1	473.7	20	1.2	76.7	19	2.8	39
Elandsberg_u*Daptocephalus*	457	14	0.4	70	41	2.1	55
Ripplemead_l*Daptocephalus*	420	25	0.3	50	11	0.4	36
Daggaboersnek_l*Daptocephalus*-2	330	78	0.5	20	1	0.1	79
Daggaboersnek_l*Daptocephalus*-1	165	55	0.3	10	5	0.5	60
Daggaboersnek_*Cistecephalus*	0	7	0.1	0	0	N/A	7
Middleton/Oudeberg_*Cistecephalus*	−100	1	0.0	0	5	N/A	6
Total specimen count		260			328		588

These relative positions were used to place tetrapod occurrences from each study area in our 13 stratigraphic bin intervals. Differences in bin interval thickness between sites relate to tectonic setting and regional thickness changes between sites (see *SI Appendix* for more information).

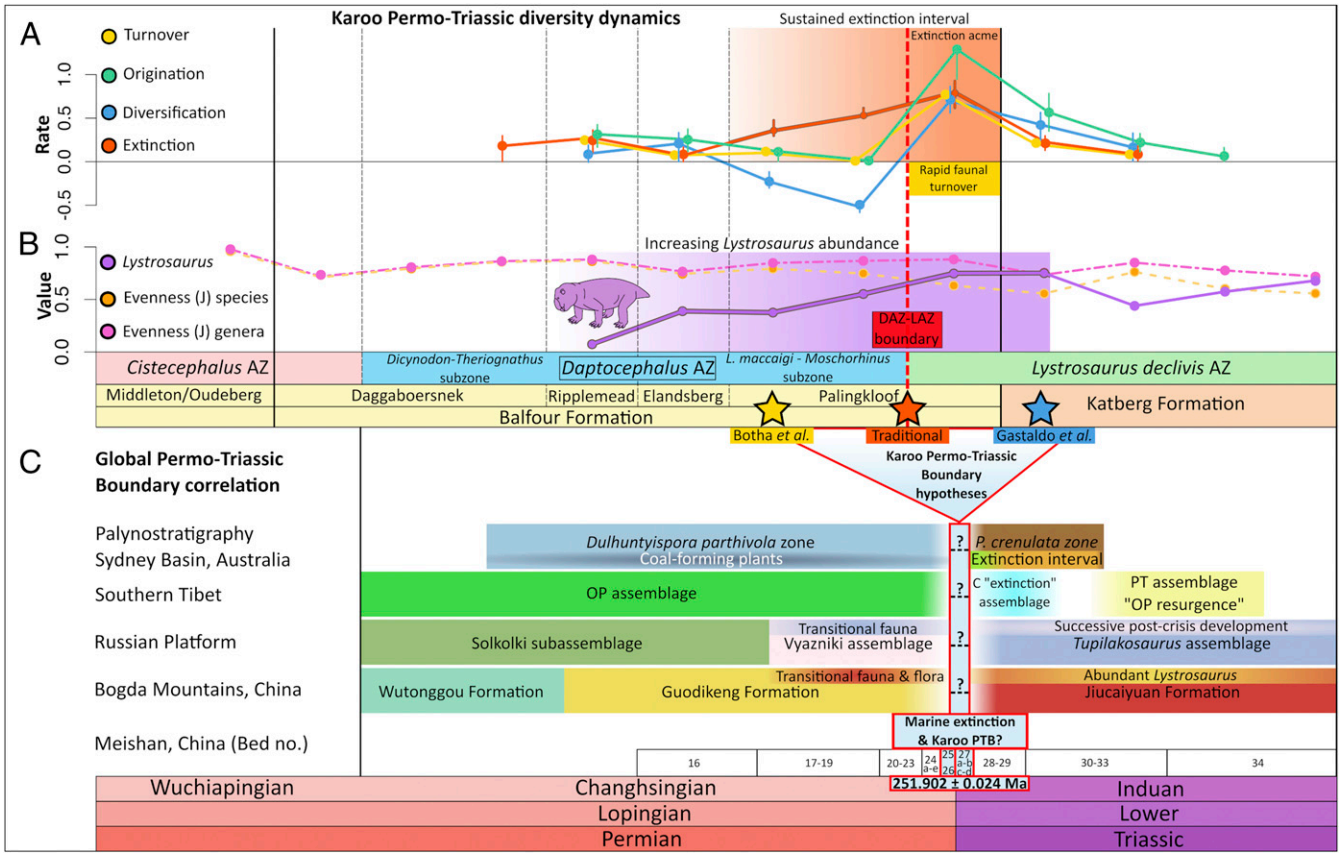

Fig. 3. (*A*) Turnover, origination, diversification, and extinction dynamics of tetrapod species across the PTT in South Africa's Karoo Basin. (*B*) Evenness (J) at species and genus resolution are shown in comparison to the genus level dominance of *Lystrosaurus*, which becomes abundant before the main extinction acme. This dominance is sustained and peaks in the post extinction interval. Rates were calculated from fossil occurrence data in 13 stratigraphic bin intervals. (*C*) Three hypotheses for the PTB placement in South Africa are compared to global PTT sections in Australia (35) but correlation to Karoo record per Gastaldo et al. (44), Russia (34), China (31, 32), and Tibet (70). Question marks (?) indicate possible placement of marine extinction at global PTT sections.

evident in the lower LAZ and again higher in the LAZ, both times coincident with peaks of *Lystrosaurus* abundance (Fig. 3*B*). Genus-level evenness shows a more prominent pattern of low values high in the LAZ and in the two bin intervals after the DAZ–LAZ boundary, co-occurring with high turnover rates (Fig. 3*B*). We regard the genus *Lystrosaurus* as an ecological group of functionally similar and closely related species, suggesting that these genus-level evenness patterns provide meaningful insights into community structure. Broadly similar results are obtained for the two-evenness metrics (*SI Appendix*, Fig. S7).

***Lystrosaurus* Abundance.** High *Lystrosaurus* abundance within its assemblage zone is well documented (46, 51, 52) and may be globally widespread by the Triassic (59). This is reflected in our study by a peak in *Lystrosaurus* abundance in the lower Katberg Formation, where ∼70% of fossil occurrences belong to *Lystrosaurus* species. Nevertheless, our data show that *Lystrosaurus* already attained high relative dominance (∼54% of all occurrences) in the Palingkloof Member of the upper DAZ, before the main extinction acme. Our data also confirm the observation (46) that two species of *Lystrosaurus* appear in the upper DAZ (*L. maccaigi*, *L. curvatus*) and another two after the main extinction acme at the base of the *Lystrosaurus declivis* Assemblage Zone (*L. declivis*, *L. murrayi*).

Discussion

The stratigraphic record of the Karoo Basin provides high-resolution data on the terrestrial end-Permian mass extinction among land vertebrates and potentially reflects the nature of the terrestrial extinction event on wider geographic scales or globally. Studies of the marine fossil record in South China (Meishan) identify a rapid extinction and fluctuating negative $\delta^{13}C$ excursions (31, 32, 35, 42, 43, 60, 61) occurring prior to and coincident with the Permo–Triassic Boundary (PTB) at 251.902 ± 0.024 Ma. The Karoo fossil record has been used as a benchmark for the continental extinction (e.g., 38–40, 51, 56). However, some studies have questioned the severity of the Karoo Permo–Triassic extinctions (55), debated the nature of environmental changes (52, 62–64), and raised uncertainties regarding their timing relative to the marine extinction and global event (e.g., 37, 40, 44, 47–49).

Our multi-index analysis of a high-resolution database of Karoo tetrapod occurrences substantially clarifies these uncertainties. We find evidence for a protracted time interval (∼1 Ma) of significantly elevated extinction rates spanning the uppermost *Daptocephalus* and lower *Lystrosaurus declivis* assemblage zones (DAZ–LAZ boundary). Therefore, we refer to the latest Permian tetrapod extinctions documented in the Karoo record as a "sustained extinction interval," and increases in sampling intensity are needed to establish whether extinctions were pulsed (39) or more gradual during this interval. Our inferences do not rely on estimating the precise timings of individual species extinctions (7, 65, 66), and at this time we recommend that this paradigm of a sustained extinction replace previous hypotheses of a single rapid extinction (42), a press-pulse extinction (43), a stepped extinction (39), or no mass extinction (55). The fact that we cannot localize tetrapod extinctions at a single stratigraphic horizon,

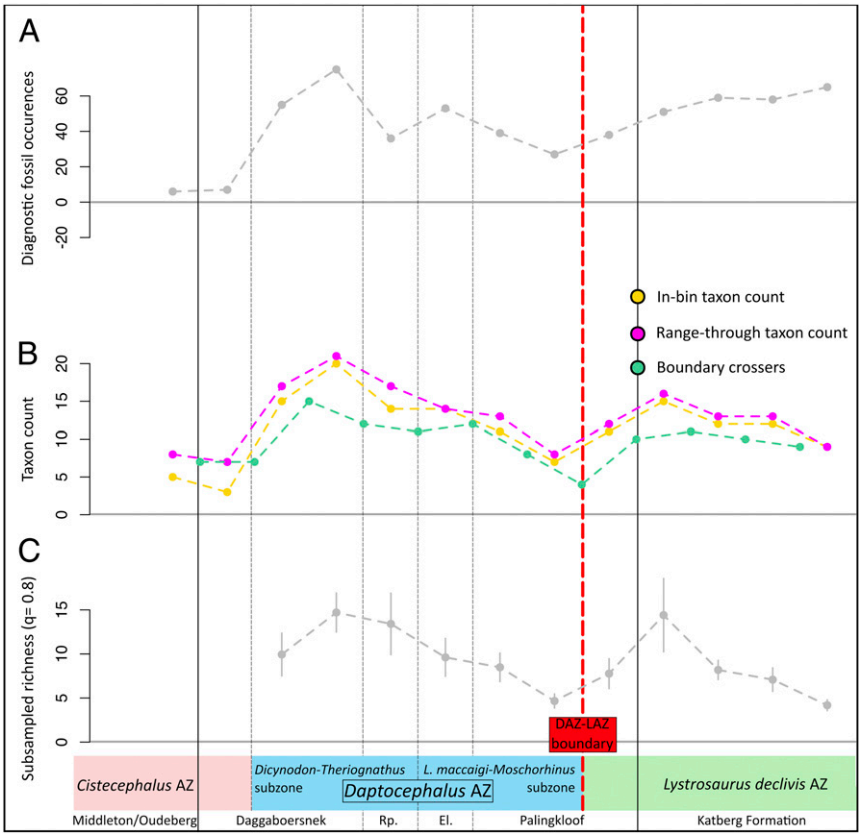

Fig. 4. (*A*) Total diagnostic fossil occurrence counts; (*B*) in bin, range through, and boundary crossers taxon counts; and (*C*) subsampled species richness calculations for the 13 Permo–Triassic stratigraphic bin intervals in our study. Red line indicates the *Daptocephalus–Lystrosaurus declivis* Assemblage Zone boundary. Rp = Ripplemead member, El = Elandsberg Member.

assemblage zone boundary, and/or PTB level does not discount the magnitude of the overall event, as reflected by the large loss of species diversity during the extinction interval and by high extinction and turnover rates. The recognition of a sustained extinction interval in the Karoo is an important advance that facilitates comparisons to extinction patterns in other coeval terrestrial sections (23, 31, 34–36, 67–70) where transitional assemblages (31, 34, 35, 70) may also indicate prolonged development of the biotic crisis followed by eventual ecosystem destabilization (Fig. 3*C*). Better correlation, quantification, and timing of these global changes to terrestrial PTT ecosystems is needed to refine models that link the ultimate causes of the end-Permian mass extinction to more localized kill mechanisms on land and in the oceans.

We found by far the highest rates of extinction, regional origination, and diversification in the upper Palingkloof Member in the lowermost LAZ above the traditional placement of the Permian–Triassic geologic boundary at the DAZ–LAZ boundary (Fig. 3*A*). If this acme of high extinction rates corresponds to the PTB then, combined with improved Permian–Triassic geochronology (37, 40, 44, 47), this suggests that the true Karoo PTB is higher in the section than its traditional placement at the DAZ–LAZ boundary and as indicated by Botha et al. (37). Nevertheless, the geochronology of Botha et al. (37) would place the onset of our sustained extinction interval closer in time to the marine extinction at the PTB (31, 32) and may therefore be conservative. By contrast, the hypothesized placement of the PTB presented by Gastaldo et al. (44), if correct, would place the entire extinction interval, and our destabilized postextinction assemblage, in the latest Permian. Regardless of geochronology, the protracted nature of the Karoo terrestrial extinction contrasts with the more rapid marine event (70).

The geochronology of Gastaldo et al. (44, 62) has been used to suggest that causal processes for the tetrapod extinctions in the Karoo were disconnected from the global mass extinction event. However, comparisons to the PTT terrestrial records from outside of South Africa in China (31), Russia (34), Australia (35), and Tibet (70) suggest a potentially similar pattern of protracted extinction and ecosystem destabilization that began in the latest Permian. Additionally, the South China Penglaitan section records an expanded record of the marine event (32), documenting two negative $\delta^{13}C$ excursions before the Penglaitan PTB extinctions [251.939 ± 0.031 Ma] in an ∼420,000 y window beginning at 252.359 ± 0.038 Ma. Similar excursions straddling the PTB on the Pingtang syncline (Nanpangian Basin, South China) are also observed by Bagherpour et al. (61), although their global significance is questioned. Shen et al. (32) propose a scenario where ecological resilience was successively diminished prior to the PTB over 420,000 y until a tipping point was reached, triggering a sudden collapse of global ecosystems. South China's marine record has generally been used as a touchstone for the definitive version of the end-Permian mass extinction event. However, our findings suggest the marine extinction may actually represent a punctuation relative to a much longer span of biological attrition on land.

The first appearances of taxa such as *Lystrosaurus declivis*, *L. murrayi*, *Prolacerta*, *Proterosuchus*, *Lydekkerina*, *Micropholis*, *Galesaurus*, *Thrinaxodon*, *Saurodektes*, and *Tetracynodon darti* in the postextinction interval have been used to posit a rapid earliest Triassic recovery for tetrapods in the Karoo (39). However, here we find that this post extinction assemblage is characterized by a co-occurrence of high extinction and origination rates, and therefore by high turnover rates, with several short-lived taxa and

overall low richness and evenness (Figs. 3*B* and 4). The question of what constitutes a "recovered" community is complex, but the abundance of four *Lystrosaurus* species combined with unusual community structures and significant community instability (11, 53, 57) suggest that postextinction ecosystems in the Karoo had not undergone a full recovery by this interval. The survival of the DAZ *Lystrosaurus* species after the main extinction acme (37) and the occurrence of potentially multiple postextinction peaks in *Lystrosaurus* abundance and low faunal evenness (Fig. 3*B*) raise the possibility that disturbed environmental conditions favoring *Lystrosaurus* species recurred or persisted for some time despite relatively high faunal diversification rates (11). Indeed, the overall lower richness, higher unevenness, and instability of these postextinction assemblages makes them similar to "disaster" faunas that have been documented in the aftermath of other mass extinctions, such as in the North American record of the Cretaceous–Paleogene extinction (70, 71). A more substantive recovery accompanied by extensive faunal turnover appears to have occurred in the Karoo by the Middle to Late Triassic *Cynognathus* Assemblage Zone (11) or potentially earlier (i.e., in the upper Katberg Formation), but high-resolution data are lacking for these assemblages.

Our findings are also consistent with the "turnover-pulse hypothesis" originally formulated by Vrba (72) to explain environment-driven bursts of speciation among African Neogene mammals between glacial and interglacial periods. This hypothesis states that climate variation causes the appearance and removal of environmental barriers to species distributions, driving pulses of extinction, and origination (turnover) interrupting longer periods of relative stasis (72). The substantial evidence for significant climatic changes related to global warming beginning at the end of the Permian period globally (16, 27, 30, 31, 35) likely had disastrous effects on local conditions in the Karoo. These effects were possibly related to aridity [(63, 64) but see ref. 62] and also increased climatic variability (52, 62). Nevertheless, it is very likely that fluctuating climates associated with the end-Permian mass extinction played a significant role in steadily altering the composition and structure of tetrapod communities in the uppermost DAZ, eventually causing an ecosystem collapse marked by the unstable, short-lived communities observed in the lower *Lystrosaurus declivis* Assemblage Zone of South Africa's Karoo Basin.

Our database and results also require a rethinking of conventional wisdom about the extinction's best-known survivor, the dicynodont synapsid *Lystrosaurus*. *Lystrosaurus* is frequently portrayed as a disaster taxon that flourished in the aftermath of the end-Permian mass extinction because of its near-global geographic range (59) and high abundance (73) as seen in the Karoo. Although "disaster taxon" is a poorly defined concept (74), the prominence of *Lystrosaurus* as a rare tetrapod example of this concept warrants detailed examination of its abundance dynamics through time. In the Karoo, it has been recognized for some time that *Lystrosaurus* first appears in traditional Permian strata alongside typical members of the upper DAZ (46, 50). However, previous studies of evenness working at assemblage zone resolution only noted a shift to *Lystrosaurus* abundance in the *Lystrosaurus declivis* Assemblage Zone (41). Our high-resolution data demonstrate that the relative abundance of *Lystrosaurus* began to increase in the Elandsberg Member of the upper DAZ and before the PTB in all age hypotheses. The relative abundance of *Lystrosaurus* increases significantly through the upper Palingkloof Member with the arrival of two additional species at the extinction acme in the upper Palingkloof Member (Fig. 3*B*) up to our post extinction interval in the uppermost Palingkloof–lowermost Katberg Formation ["recovery phase" of Botha et al. (39)]. Its abundance then decreases slightly in the lowermost portions of the Katberg Formation before increasing again. The pattern of early increase in *Lystrosaurus* abundance is similar to that of *Diictodon*, a common Permian dicynodont and disaster taxon-like survivor whose abundance steadily increased across the end-Guadalupian extinction acme in the Karoo Basin (75).

The paleobiological insights *Lystrosaurus* can provide are also intriguing, as juvenile aggregation during adverse conditions (52), burrowing, growth and life history patterns (76), feeding system biomechanics (77), and broad environmental tolerance (78) have all been factors suggested to contribute to its success. Although our data do not allow us to determine which, if any, of these factors was of greatest importance, they do indicate that *Lystrosaurus* was able to take advantage of changing environmental and ecological conditions before the PTT in a way that other taxa, including its contemporary dicynodont relatives, could not. Therefore, the success of *Lystrosaurus* and the likely reason for its cosmopolitan distribution was not caused strictly by the ecological aftermath of the PTT or Early Triassic environments but instead had its roots in the Permian. A similar ability to benefit from the conditions that create and sustain mass extinctions may be common among disaster taxa in general, and testing this hypothesis will require greater scrutiny of high-resolution occurrence datasets.

Our high-resolution, multi-index approach significantly refines understanding of tetrapod extinctions during the PTT in the Karoo Basin, providing a quantitative picture of extinctions on land that is possibly representative of the global record. Replacing the abrupt or stepwise narratives of the event with a protracted period of sustained extinction followed by rapid species turnover is a key step in correlating the biotic crisis in the Karoo with regional and global environmental changes, revised geochronology, and the record of extinctions preserved in other areas that may also provide evidence for successive extinctions and the occurrence of transitional communities (32, 34, 35, 70). The rise of the disaster taxon *Lystrosaurus* well before the Permian–Triassic boundary indicates that its success did not stem solely from an ability to survive postextinction conditions. Instead, it likely had preexisting adaptations or ecological and evolutionary versatility that allowed it to flourish under the conditions that caused widespread and sustained extinctions among other taxa. We observe a phase of rapid speciation and turnover in the post extinction aftermath, suggestive of a destabilized ecosystem, and possibly also reflected in the floral record of Australia (35) and Tibet (70). This period of instability was likely key to breaking the incumbency of previously dominant synapsid clades, paving the way for the rise of archosaurs and their relatives as a more complete recovery was achieved later in the Triassic. Finally, the changing narrative of PTT extinctions in the Karoo emphasizes that a more nuanced approach to the end-Permian mass extinction is needed that accounts for the idiosyncrasies of the event in different geographical areas. Only by recognizing the specific details of the extinction in different places can the search for generalizations be successful.

Materials and Methods

Our study area encompasses two sites from South Africa's south central Karoo region named Site A (Graaff-Reinet and Nieu Bethesda) and Site B (Bethulie and Gariep Dam) (Fig. 1). Additional site map figures can be found in *SI Appendix*, Figs. S1 and S2). Regional variation in lithostratigraphic thickness documented by Viglietti et al. (56, 79) at these sites necessitates that we index species occurrences using relative position in local lithostratigraphic units, and the definitions of these units were refined by Viglietti et al. (79) (*SI Appendix*). These lithostratigraphic refinements were used to assign taxa to stratigraphic bin intervals on classic stratigraphic sections measured at these sites (37, 39, 56, 79) (*SI Appendix*, Figs. S3–S5). Many fossil specimens in this study were collected at or close to these stratigraphic section locations and were used to document numbers of occurrences within bins (Table 1). This work allowed us to analyze a dataset comprising 588 tetrapod fossil specimens lithostratigraphically resolved at meter-level precision (Table 1). More information on how the information in Table 1 was obtained can be found in *SI Appendix*. For more information on raw metadata for fossil species occurrences, see Dataset S1. Specimen data for these occurrences includes accession and/or field number, species identification,

location (farm name and centroid), quarry, and stratigraphic position (meter, lithostratigraphic, and bin interval position).

Dataset S1 is the collation and extension of two previous datasets compiled by Van der Walt et al. (73) (historic collections) and more recent fossil collections (37, 39, 56). Where possible, specimens had their provenance data refined by referring to relevant literature and historic field notes. Any specimens not collected and those lacking confirmed identifications were discarded from the study. The 588 specimens primarily represent singleton fossil finds (unless specified, see Dataset S1) and comprise 53 species that occur in the Middleton, Balfour, and lower Katberg formations and span a time interval of ∼4 My based on the isotope dilution–thermal ionization mass spectrometry age of Rubidge et al. (80) (Fig. 1). The positions of 124 specimens in the supplementary dataset of ref. 39 were identified as being incongruent by ref. 49. We corrected these here (Dataset S2). Many were correctly placed on previously published sections, and the inconsistent data presented in ref. 39 result from transcription errors (figure 4 in ref. 39). Our analyses were conducted at the level of occurrences of species within localities (i.e., quarries or bonebeds representing a single stratigraphic horizon within a localized area). Therefore, multiple specimens (individuals) representing just one species from a single locality were analyzed as being one single occurrence of that species.

All species occurrences used in our study had their identifications confirmed by taxonomic experts including K.D.A. and C.F.K. The ranges and occurrence counts of vertebrate species in our 13 stratigraphic bin intervals are shown in Fig. 2. For certain species, uncertain occurrences are shown on the range chart but were not included in the analyses. We divided the species occurrences into 13 stratigraphic bins, which represent an average of 300,000 y each. The average age range for each bin was calculated using the estimated age duration of our study (∼4 Ma). A total of 13 bin intervals were constructed to balance approximate temporal duration and tectonic setting (79) with minimum numbers of specimens per bin after excluding the most frequent species. Differences in the absolute age measurements presented by refs. 37 and 47 create $\sim \pm 0.1$ Ma uncertainty to our age estimate for bins straddling the PTT. Improved geochronology is needed to refine the bin interval models presented in this study.

We analyzed the high-resolution data (i.e., those occurrences with lithostratigraphic positions known to within meter-level resolution) using shareholder quorum subsampling (SQS, or coverage-based rarefaction) (81, 82) to estimate richness [the R package iNext version 2.0.20; Hsieh et al. (83)] and the modified version of the gap-filler method (84) for inferring rates of extinction and origination while accounting for variation in sampling rate (custom code in R version 4.0.0; Dataset S3). Species occurrences within each stratigraphic bin were subsampled to a uniform count of $n = 19$ prior to computation of extinction and origination (84), and we summarized the results from 1,000 iterations as the median and interquartile range in our results figures. Diversification rates were calculated as origination rate minus extinction rate, and turnover was calculated as the smaller value of either extinction or origination rate within each bin, representing the approximate amount of extinction that was balanced by origination (i.e., turnover). We implemented SQS at a quorum of 0.8 (Fig. 3*A*) and in our supplement (*SI Appendix*, Fig. S6) also show results at a wider range of quora and excluding the dominant (most frequent) species or pair of species from each interval prior to calculation to reduce the biasing effects of variation in evenness (e.g., ref. 5). We also quantified evenness using Pielou's J and the Evar metric using the R package Codyn version 2.0.4 (85) (*SI Appendix*, Fig. S7) at both species and genus levels and the proportion of occurrences belonging to *Lystrosaurus* species within each interval. Our analyses infer the pattern of extinction and turnover across all our studied intervals rather than assuming coincidence with the Permian–Triassic geologic boundary.

Data Availability. All study data are included in the article and/or supporting information.

ACKNOWLEDGMENTS. P.A.V. thanks the Field Museum's Women in Science Board and the Grainger Bioinformatics Center for their generous support. We are thankful for assistance by staff at the Evolutionary Studies Institute (Mr. Wilfred Bilankulu, Prof. Jonah Choiniere, Mr. Charlton Dube, Mr. Gerry Germishuizen, Mr. Sifelani Jirah, Mr. Gilbert Mokgethoa, Ms. Gladys Mokoma, Mr. Pepson Mukanela, Mr. Thilivhali Nemavhundi, and Dr. Bernhard Zipfel), Iziko South African Museum (Ms. Claire Browning), National Museum, and the Albany Museum (Dr. Rose Prevec and Prof. Billy de Klerk). We also thank the editor and three anonymous reviewers for greatly improving the final manuscript.

1. S. Finnegan, N. A. Heim, S. E. Peters, W. W. Fischer, Climate change and the selective signature of the Late Ordovician mass extinction. *Proc. Natl. Acad. Sci. U.S.A.* **109**, 6829–6834 (2012).
2. D. P. Bond, P. B. Wignall, Large igneous provinces and mass extinctions: An update. *Geol. Soc. Am. Bull.* **505**, 29–55 (2014).
3. L. W. Alvarez, W. Alvarez, F. Asaro, H. V. Michel, Extraterrestrial cause for the Cretaceous-Tertiary extinction. *Science* **208**, 1095–1108 (1980).
4. P. Schulte *et al*., The Chicxulub asteroid impact and mass extinction at the Cretaceous-Paleogene boundary. *Science* **327**, 1214–1218 (2010).
5. J. Alroy, The shifting balance of diversity among major marine animal groups. *Science* **329**, 1191–1194 (2010).
6. P. Hull, Life in the aftermath of mass extinctions. *Curr. Biol.* **25**, R941–R952 (2015).
7. M. Foote, Origination and extinction through the Phanerozoic: A new approach. *J. Geol.* **111**, 125–148 (2003).
8. M. Foote, D. M. Raup, Fossil preservation and the stratigraphic ranges of taxa. *Paleobiology* **22**, 121–140 (1996).
9. D. M. Raup, J. J. Sepkoski Jr, Mass extinctions in the marine fossil record. *Science* **215**, 1501–1503 (1982).
10. R. A. Close *et al*., Diversity dynamics of Phanerozoic terrestrial tetrapods at the local-community scale. *Nat. Ecol. Evol.* **3**, 590–597 (2019).
11. P. D. Roopnarine, K. Angielczyk, A. Weik, A. Dineen, Ecological persistence, incumbency and reorganization in the Karoo Basin during the Permian-Triassic transition. *Earth Sci. Rev.* **189**, 244–263 (2019).
12. S. Sahney, M. J. Benton, Recovery from the most profound mass extinction of all time. *Proc. Biol. Sci.* **275**, 759–765 (2008).
13. E. Petsios, D. J. Bottjer, Quantitative analysis of the ecological dominance of benthic disaster taxa in the aftermath of the end-Permian mass extinction. *Paleobiology* **42**, 380–393 (2016).
14. D. M. Raup, J. J. Sepkoski Jr, Periodicity of extinctions in the geologic past. *Proc. Natl. Acad. Sci. U.S.A.* **81**, 801–805 (1984).
15. P. Wignall, The End-Permian mass extinction–how bad did it get? *Geobiology* **5**, 303–309 (2007).
16. M. J. Benton, A. J. Newell, Impacts of global warming on Permo-Triassic terrestrial ecosystems. *Gondwana Res.* **25**, 1308–1337 (2014).
17. W. Kiessling, C. Simpson, On the potential for ocean acidification to be a general cause of ancient reef crises. *Glob. Change Biol.* **17**, 56–67 (2011).
18. A. H. Knoll, R. K. Bambach, J. L. Payne, S. Pruss, W. W. Fischer, Paleophysiology and end-Permian mass extinction. *Earth Planet. Sci. Lett.* **256**, 295–313 (2007).
19. S. M. Stanley, Estimates of the magnitudes of major marine mass extinctions in earth history. *Proc. Natl. Acad. Sci. U.S.A.* **113**, E6325–E6334 (2016).
20. J. Fedorowski, Extinction of Rugosa and Tabulata near the Permian/Triassic boundary. *Acta Palaeontol. Pol.* **34**, 47–70 (1989).
21. X.-D. Wang, X.-J. Wang, Extinction patterns of late Permian (Lopingian) corals in China. *Palaeoworld* **16**, 31–38 (2007).
22. A. Brayard *et al*., Good genes and good luck: Ammonoid diversity and the end-Permian mass extinction. *Science* **325**, 1118–1121 (2009).
23. S. Mishra, N. Jha, A. Stebbins, M. Brookfield, R. Hannigan, Palaeoenvironments, flora, and organic carbon and nitrogen isotope changes across the non-marine Permian-Triassic boundary at Wybung Head, Australia. *Palaeogeogr. Palaeoclimatol. Palaeoecol.* **534**, 109292 (2019).
24. G. J. Retallack, J. J. Veevers, R. Morante, Global coal gap between Permian–Triassic extinction and Middle Triassic recovery of peat-forming plants. *Geol. Soc. Am. Bull.* **108**, 195–207 (1996).
25. J. M. Schopf, "Forms and facies of Vertebraria in relation to Gondwana coal" in *Geology of the Central Transantarctic Mountains Antarctic Research Series* (American Geophysical Union, 1986), vol. 36, pp. 37–62.
26. Z.-Q. Chen, M. J. Benton, The timing and pattern of biotic recovery following the end-Permian mass extinction. *Nat. Geosci.* **5**, 375–383 (2012).
27. Y. Sun *et al*., Lethally hot temperatures during the Early Triassic greenhouse. *Science* **338**, 366–370 (2012).
28. D. J. Bottjer, Geochemistry. Life in the Early Triassic ocean. *Science* **338**, 336–337 (2012).
29. M. J. Benton, R. J. Twitchett, How to kill (almost) all life: The end-permian extinction event. *Trends Ecol. Evol.* **18**, 358–365 (2003).
30. D. H. Erwin, *Extinction: How Life on Earth Nearly Ended 250 Million Years Ago* (Princeton University Press, New Jersey, 2006).
31. I. Metcalfe *et al*., Stratigraphy, biostratigraphy and C-isotopes of the Permian–Triassic non-marine sequence at Dalongkou and Lucaogou, Xinjiang province, China. *J. Asian Earth Sci.* **36**, 503–520 (2009).
32. S.-Z. Shen *et al*., A sudden end-Permian mass extinction in South China. *Geol. Soc. Am. Bull.* **131**, 205–223 (2019).
33. M. Brookfield, T. Algeo, R. Hannigan, J. Williams, G. Bhat, Shaken and stirred: Seismites and tsunamites at the Permian-Triassic boundary, Guryul Ravine, Kashmir, India. *Palaios* **28**, 568–582 (2013).
34. A. Sennikov, V. Golubev, Vyazniki biotic assemblage of the terminal Permian. *Paleontol. J.* **40**, S475–S481 (2006).
35. C. R. Fielding *et al*., Age and pattern of the southern high-latitude continental end-Permian extinction constrained by multiproxy analysis. *Nat. Commun.* **10**, 385 (2019).
36. G. Retallack *et al*., The Permian–Triassic boundary in Antarctica. *Antarct. Sci.* **17**, 241–258 (2005).

37. J. Botha *et al*., New geochemical and palaeontological data from the Permo-Triassic boundary in the South African Karoo Basin test the synchronicity of terrestrial and marine extinctions. *Palaeogeogr. Palaeoclimatol. Palaeoecol.* **540**, 109467 (2020).
38. J. Botha-Brink, A. K. Huttenlocker, S. P. Modesto, "Vertebrate paleontology of Nooitgedacht 68: A *Lystrosaurus maccaigi*-rich Permo-Triassic Boundary locality in South Africa" in *Early Evolutionary History of the Synapsida*, C. F. Kammerer, K. D. Angielczyk, J. Fröbisch, Eds. (Springer Netherlands, 2014), pp. 289–304.
39. R. M. H. Smith, J. Botha-Brink, Anatomy of a mass extinction: Sedimentological and taphonomic evidence for drought-induced die-offs at the Permo-Triassic boundary in the main Karoo Basin, South Africa. *Palaeogeogr. Palaeoclimatol. Palaeoecol.* **396**, 99–118 (2014).
40. P. A. Viglietti, R. M. Smith, B. S. Rubidge, Changing palaeoenvironments and tetrapod populations in the *Daptocephalus* Assemblage Zone (Karoo Basin, South Africa) indicate early onset of the Permo-Triassic mass extinction. *J. Afr. Earth Sci.* **138**, 102–111 (2018).
41. R. B. Irmis, J. H. Whiteside, Delayed recovery of non-marine tetrapods after the end-Permian mass extinction tracks global carbon cycle. *Proc. Biol. Sci.* **279**, 1310–1318 (2012).
42. R. M. H. Smith, P. D. Ward, Pattern of vertebrate extinctions across an event bed at the Permian-Triassic boundary in the Karoo Basin of South Africa. *Geology* **29**, 1147–1150 (2001).
43. P. D. Ward *et al*., Abrupt and gradual extinction among Late Permian land vertebrates in the Karoo basin, South Africa. *Science* **307**, 709–714 (2005).
44. R. A. Gastaldo *et al*., The base of the *Lystrosaurus* Assemblage Zone, Karoo Basin, predates the end-Permian marine extinction. *Nat. Commun.* **11**, 1428 (2020).
45. J. Botha, R. M. H. Smith, Rapid vertebrate recuperation in the Karoo Basin of South Africa following the End-Permian extinction. *J. Afr. Earth Sci.* **45**, 502–514 (2006).
46. J. Botha, R. M. H. Smith, *Lystrosaurus* species composition across the Permo–Triassic boundary in the Karoo Basin of South Africa. *Lethaia* **40**, 125–137 (2007).
47. R. A. Gastaldo *et al*., Is the vertebrate-defined Permian-Triassic boundary in the Karoo Basin, South Africa, the terrestrial expression of the end-Permian marine event? *Geology* **43**, 1–5 (2015).
48. R. A. Gastaldo, J. Neveling, C. K. Clark, S. S. Newbury, The terrestrial Permian-Triassic boundary event bed is a nonevent. *Geology* **37**, 199–202 (2009).
49. R. A. Gastaldo, J. Neveling, J. W. Geissman, C. V. Looy, Testing the *Daptocephalus* and *Lystrosaurus* assemblage zones in a lithostratigraphic, magnetostratigraphic, and palynological framework in the Free State, South Africa. *Palaios* **34**, 542–561 (2019).
50. R. M. H. Smith, Changing fluvial environments across the Permian-Triassic boundary in the Karoo Basin, South Africa and possible causes of tetrapod extinctions. *Palaeogeogr. Palaeoclimatol. Palaeoecol.* **117**, 81–104 (1995).
51. R. M. H. Smith, J. Botha, The recovery of terrestrial vertebrate diversity in the South African Karoo Basin after the end-Permian extinction. *C. R. Palevol* **4**, 623–636 (2005).
52. P. A. Viglietti, R. M. H. Smith, J. Compton, Origin and palaeoenvironmental significance of *Lystrosaurus* bonebeds in the earliest Triassic Karoo Basin, South Africa. *Palaeogeogr. Palaeoclimatol. Palaeoecol.* **392**, 9–21 (2013).
53. P. D. Roopnarine *et al*., Comparative ecological dynamics of Permian-Triassic communities from the Karoo, Luangwa, and Ruhuhu Basins of southern Africa. *J. Vertebr. Paleontol.* **37**, 254–272 (2018).
54. C. A. Sidor *et al*., Provincialization of terrestrial faunas following the end-Permian mass extinction. *Proc. Natl. Acad. Sci. U.S.A.* **110**, 8129–8133 (2013).
55. S. G. Lucas, *Permian Tetrapod Biochronology, Correlation and Evolutionary Events* (Geological Society, London, Special Publications, London, 2017), vol. 450, pp. 405–444.
56. P. A. Viglietti *et al*., The *Daptocephalus* assemblage zone (Lopingian), South Africa: A proposed biostratigraphy based on a new compilation of stratigraphic ranges. *J. Afr. Earth Sci.* **113**, 153–164 (2016).
57. P. Roopnarine, K. Angielczyk, *The Stability of Ecological Communities as an Agent of Evolutionary Selection: Evidence from the Permian-Triassic Mass Extinction. Evolutionary Theory: A Hierarchical Perspective* (University of Chicago Press, Chicago, IL, 2016), pp. 307–333.
58. J. Fröbisch, "Synapsid diversity and the rock record in the Permian-Triassic Beaufort Group (Karoo Supergroup), South Africa" in *Early Evolutionary History of the Synapsida*, C. F. Kammerer, K. D. Angielczyk, J. Fröbisch, Eds. (Springer, 2014), pp. 305–319.
59. J. Fröbisch, Composition and similarity of global anomodont-bearing tetrapod faunas. *Earth Sci. Rev.* **95**, 119–157 (2009).
60. M. B. Steiner, Y. Eshet, M. R. Rampino, D. M. Schwindt, Fungal abundance spike and the Permian–Triassic boundary in the Karoo supergroup (South Africa). *Palaeogeogr. Palaeoclimatol. Palaeoecol.* **194**, 405–414 (2003).
61. B. Bagherpour *et al*., Are Late Permian carbon isotope excursions of local or of global significance? *Geol. Soc. Am. Bull.* **132**, 521–544 (2020).
62. R. A. Gastaldo, N. Tabor, J. Neveling, Trends in stable-isotopes and climate proxies from late Changhsingian ghost landscapes of the Karoo Basin, South Africa. *Front. Ecol. Evol.* **8**, 1–18 (2020).
63. K. G. MacLeod, P. C. Quinton, D. J. Bassett, Warming and increased aridity during the earliest Triassic in the Karoo Basin, South Africa. *Geology* **45**, 483–486 (2017).
64. K. Rey *et al*., Global climate perturbations during the Permo-Triassic mass extinctions recorded by continental tetrapods from South Africa. *Gondwana Res.* **37**, 384–396 (2016).
65. P. M. Hull, S. A. Darroch, D. H. Erwin, Rarity in mass extinctions and the future of ecosystems. *Nature* **528**, 345–351 (2015).
66. P. W. Signor, J. H. Lipps, L. Silver, P. Schultz, "Sampling bias, gradual extinction patterns, and catastrophes in the fossil record" in *Geological Society of America Special Paper 190* (Geological Society of America, 1982), pp. 291–296.
67. V. Davydov *et al*., Radioisotopic and biostratigraphic constraints on the classical Middle–Upper Permian succession and tetrapod fauna of the Moscow syneclise, Russia. *Geology* **48**, 742–747 (2020).
68. Z. Feng *et al*., From rainforest to herbland: New insights into land plant responses to the end-Permian mass extinction. *Earth Sci. Rev.* **204**, 103153 (2020).
69. M. R. Rampino, K. Caldeira, A. Prokoph, "What causes mass extinctions? Large asteroid/comet impacts, flood-basalt volcanism, and ocean anoxia — Correlations and cycles" in *Geological Society of America Special Paper 542* (Geological Society of America, 2019), pp. 271–302.
70. F. Liu *et al*., Palynology and vegetation dynamics across the Permian–Triassic boundary in southern Tibet. *Earth Sci. Rev.* **209**, 103278 (2020).
71. S. M. Smith *et al*., Early mammalian recovery after the end-cretaceous mass extinction: A high-resolution view from McGuire creek area, Montana, USA. *Bulletin* **130**, 2000–2014 (2018).
72. E. S. Vrba, Environment and evolution: Alternative causes of the temporal distribution of evolutionary events. *S. Afr. J. Sci.* **81**, 229–236 (1985).
73. M. van der Walt, M. O. Day, B. S. Rubidge, A. K. Cooper, I. Netterberg, A new GIS-based biozone map of the Beaufort group (Karoo supergroup), South Africa. *Palaeontologia Africana* **45**, 1–5 (2011).
74. S. P. Modesto, The disaster taxon *Lystrosaurus*: A paleontological myth. *Front. Earth Sci.* **8**, 610463 (2020).
75. M. O. Day, R. B. Benson, C. F. Kammerer, B. S. Rubidge, Evolutionary rates of mid-Permian tetrapods from South Africa and the role of temporal resolution in turnover reconstruction. *Paleobiology* **44**, 347–367 (2018).
76. J. Botha, The paleobiology and paleoecology of South African *Lystrosaurus*. *PeerJ* **8**, e10408 (2020).
77. S. C. Jasinoski, E. J. Rayfield, A. Chinsamy, Mechanics of the scarf premaxilla-nasal suture in the snout of *Lystrosaurus*. *J. Vertebr. Paleontol.* **30**, 1283–1288 (2010).
78. M. R. Whitney, C. A. Sidor, Evidence of torpor in the tusks of *Lystrosaurus* from the early triassic of Antarctica. *Commun. Biol.* **3**, 471 (2020).
79. P. A. Viglietti, B. S. Rubidge, R. M. H. Smith, New late Permian tectonic model for South Africa's Karoo Basin: Foreland tectonics and climate change before the end-Permian crisis. *Sci. Rep.* **7**, 10861 (2017).
80. B. S. Rubidge, D. H. Erwin, J. Ramezani, S. A. Bowring, W. J. de Klerk, High-precision temporal calibration of late Permian vertebrate biostratigraphy: U-Pb zircon constraints from the Karoo supergroup, South Africa. *Geology* **10**, 1–4 (2013).
81. J. Alroy, "Fair sampling of taxonomic richness and unbiased estimation of origination and extinction rates" in Quantitative Methods in Paleobiology, Paleontological Society Short Course at the Annual Meeting of the Geological Society of America, 16, J. Alroy, G. Hunt, Eds. (Geological Society of America, 2010), pp. 55–80.
82. A. Chao, L. Jost, Coverage-based rarefaction and extrapolation: Standardizing samples by completeness rather than size. *Ecology* **93**, 2533–2547 (2012).
83. T. Hsieh, K. Ma, A. Chao, M. T. Hsieh, Package 'iNEXT' (2016). http://chao.stat.nthu.edu.tw/wordpress/software_download/. Accessed 28 February 2017.
84. J. Alroy, A more precise speciation and extinction rate estimator. *Paleobiology* **41**, 633–639 (2015).
85. L. M. Hallett *et al*., codyn: An R package of community dynamics metrics. *Methods Ecol. Evol.* **7**, 1146–1151 (2016).